ECCM21 – 21st European Conference on Composite Materials
02-05 July 2024, Nantes, France
DOI : 10.60691/yj56-np80
https://gem.ec-nantes.fr/en/eccm21-proceedings/

AN AUTOMATED REMESHING ALGORITHM FOR THE NUMERICAL ANALYSIS OF PROPAGATING DELAMINATIONS

Luca M. Martulli[1], Leonardo Guido Salvi[1] and Andrea Bernasconi[1]

[1]Department of Mechanical Engineering, Politecnico di Milano, Via La Masa 1, I-20156 Milano, Italy
Email: lucamichele.martulli@polimi.it

Keywords: Delaminations, Numerical modelling, Virtual Crack Closure Technique

Abstract
Delaminations are a critical failure mode for composite laminates. The Virtual Crack Closure Technique (VCCT) is a useful tool to analyse propagating delaminations in numerical simulations. However, it is a mesh dependent technique: when the mesh is not conformal to the delamination front, incorrect calculations of the strain energy release rate are possible. This has severely affected the applicability of VCCT to complex cases with large and curved crack fronts. In this work, we implemented an automated remeshing algorithm capable of creating meshes that are always conformal to the delamination front. The algorithm was implemented using a sequential-simulation approach: several simulations are launched, where each simulation is automatically prepared and launched based on the results of the previous. This was shown to accelerate significantly the computational time required. The developed algorithm was able to eliminate the numerical errors due to the non-conformity between the mesh and the delamination front. Discrepancies from the considered experimental reference case are still present, but can be further investigated thanks to the versatility of the sequential-simulation approach. This work sets the basis for such further development of the remeshing algorithm and its implementation in a fatigue modelling approach.

1. Introduction

Delaminations are among the primary causes of failures in laminated fibre reinforced composites. These defects consist of cracks occurring between the layers of cured laminates, where the composite tend to be weaker. The experimental effort on the topic lead to the development of different numerical tools to model delamination propagating in laminated parts. Among these tools, the Virtual Crack Closure Technique (VCCT) is among the most effective and commonly used [1].

The VCCT is a numerical technique implemented in several finite element software: it requires two meshed parts sharing an interface along which a crack will (or will not) eventually propagate. At the interface, the corresponding nodes of the two parts generally coincide and, when the interface is undamaged, they are bonded together. A node-by-node computation of the Strain Energy Release Rate (SERR) $\mathcal{G}$ is then performed: the nodes for which the computed $\mathcal{G}$ is higher than the material fracture toughness $\mathcal{G}_c$, the nodes of the two parts are separated and a crack is formed. Depending on the local coordinate system of the crack, $\mathcal{G}$ can be decomposed in its mode I, mode II and mode III contribution, namely $\mathcal{G}_I$, $\mathcal{G}_{II}$ and $\mathcal{G}_{III}$, respectively.

The VCCT offers several advantages over other techniques and represents a useful tool for composite laminates' design and analysis. However, it is also affected by some limitations. Among these, the technique is inherently mesh dependent, since the delamination front is described via bonded or unbonded nodes, rather than elements. The node discretisation is especially weak when large and curved delamination fronts are encountered: in these cases, the fronts is usually not conformal to the mesh.

DOI : 10.60691/yj56-np80
https://gem.ec-nantes.fr/en/eccm21-proceedings/

Martulli and Bernasconi highlighted a SERR concentration effect when a curved front was modelled as a stepped front [2].

This work aims to simulate a large and curved delamination front propagating in a composite laminate by eliminating the SERR concentration effect. To this end, an automated remeshing algorithm was developed and implemented in a sequential simulation approach. This approach, previously developed for fatigue simulations, is based on a series of consecutive simulations: each simulation is prepared based on the results of the previous and launched automatically. In this work, a single static load ramp is divided into several simulations of smaller load increments; between each simulation, the mesh of the different parts is updated to ensure its conformity with the delamination front. A partially reinforced Double Cantilever Beam (DCB) specimen [3] was considered as validation case, as it presents a large delamination front evolving in different curved shapes.

2. Materials and methods

2.1. Code structure and explanation

The developed approach splits a single mechanical simulation into multiple ones. Consider P_{max} as the maximum applied load (or displacement) to be applied. The load P_{max} is then applied incrementally in n_{sim} simulations: the load applied in each simulation is thus:

$$P_i = i \cdot \frac{P_{max}}{n_{sim}} = i \cdot \Delta P \tag{1}$$

where P_i is the load for the i-th simulation.

The remeshing algorithm exploits the Python scripting capabilities of Abaqus: a single master Python script prepares, launches and extract results from each simulation. Figure 1 shows the structure of the developed code. As shown, the required inputs to the Python code are: i) the properties of the interface where the delamination occurs: the fracture toughnesses $\mathcal{G}_{Ic}$, $\mathcal{G}_{IIc}$ and $\mathcal{G}_{IIIc}$ and the parameter η of the BK law [4]; ii) the numerical inputs for the sequential simulations: the maximum applied load P_{max}, respectively, the nodal distance d_n (that is the element length at the interface), the degree of interpolating polynomial n_{poly} and the number of simulations n_{sim} to be performed; iii) the Abaqus model to be analysed. In the Abaqus model, the nodes belonging to the delaminating interface must be separated into two complementary sets: the bonded and the debonded nodes. All other necessary inputs (material properties, boundary conditions, etc.) are defined inside the prepared Abaqus model. In this work, Abaqus 2021 version was used [5].

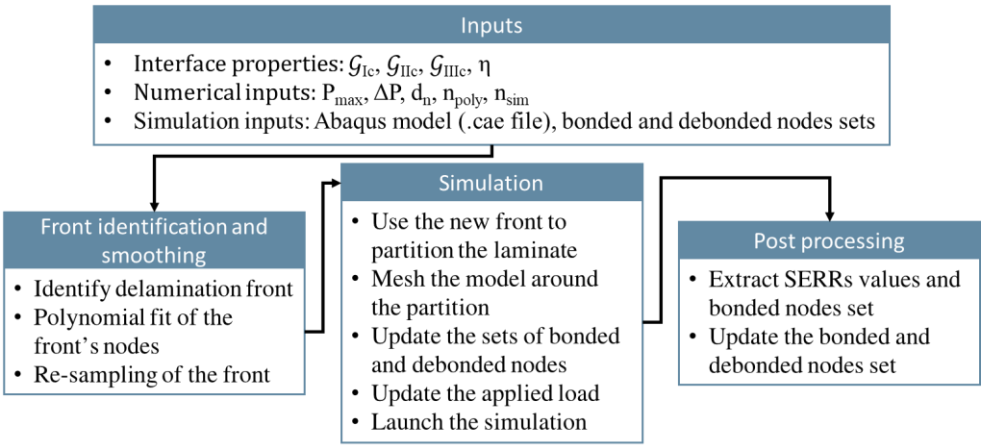

Figure 1. Structure of the developed code.

DOI : 10.60691/yj56-np80
https://gem.ec-nantes.fr/en/eccm21-proceedings/

To ensure the conformity between the mesh and the delamination front, the latter must be propertly identified. This is done by evaluating, for each bonded node, the distance with the other debonded nodes. If the minimum distance (i.e. the distance from the closer node) is smaller than $k \cdot d_n$, the node belongs to the delamination front. The constant k is used to ensure that small variations of the mesh size do not affect significantly the front identification. In this work, k is set to 1.2. Note that this front identification strategy works best for regular meshes where little variations of d_n occurs.

The delamination front is thus identified via its nodes, which makes its description discontinuous. The front is thus smoothed via a polynomial fit to obtain a continuous function. The adopted polynomial is of degree n_{poly}: a degree of 12 was found suited for the present work. The polynomial is then resampled with equal spacing, to obtain a nodal discontinuous description of the smoothed front.

The Python script copies the original Abaqus model into a new one, with its parts, material properties, boundary conditions and load cases. The composite laminates between which the delamination occurs are partitioned using the new smoothed delamination front. A partition in the geometry will force the mesh to adapt and conform to the front line, ensuring a more orthogonal mesh; moreover, the points resampled on the new delamination front will serve as mesh seed. A new mesh is thus generated on the composite laminates. Moreover, the applied load is set to P_i for the i-th simulation, following Eq. 1. Finally, the simulation is launched.

The Python script waits for the end of the simulation. Once the simulation is finished, the script automatically opens the output file (.odb file) and: i) extracts the values of $\mathcal{G}_{\mathrm{I}}$, $\mathcal{G}_{\mathrm{II}}$ and $\mathcal{G}_{\mathrm{III}}$ for the bonded nodes; ii) in case any node debonded during the simulation, it updates the sets of bonded and unbonded nodes.

2.2. Experimental validation case

The developed approach was tested on the partially reinforced DCB specimen reported in [3]. This was selected because it presents a large and curved delamination front. Moreover, this was the validation case for a sequential algorithm for fatigue predictions in a prior work [2]: the inaccuracies in the SERR evaluation caused by the non-orthogonality between the mesh and the delamination front seemed to have caused severe discrepancies from the experimental case.

Figure 2 shows the modelled geometry of the partially reinforced DCB. As shown, each arm of the DCB is composed by a large plate (dimensions 175 mm x 60 mm x 1.51 mm) and a smaller plates (dimensions 42.5 mm x 120 mm x 1.51 mm) bonded on top of the former. Both plates are made by 8 unidirectional plies of carbon fibre/epoxy oriented at 0° (aligned with the X-axis in Figure 2). The material properties are reported in Table 1. The initial mesh sized adopted was 0.5 mm in the delamination propagation region, while 1.5 mesh was used elsewhere. Continuum shell elements were used, implying the use of one element in the thickness per each plate. Finally, Figure 2 also shows the applied boundary conditions on the two DCBs' arms. As shown, finite stiffness springs were used (elastic stiffness equal to 1562 N/mm) to take into account the stiffness of the testing fixture (as done in [2,6]). The mesh considered is the same as the one adopted in [2], to which the reader is then referred to for further details. Moreover, further details on the simulated static tests are available at [3].

Two types of simulations are performed. First, to assess the algorithm effectiveness in removing the SERR concentrations, an experimental delamination front was considered and smoothed as described in Section 2.1. The selected experimental front is the one corresponding to an applied opening displacement of 4 mm. For this analysis, unrealistically high fracture toughnesses $\mathcal{G}_{\mathrm{Ic}}$, $\mathcal{G}_{\mathrm{IIc}}$ and $\mathcal{G}_{\mathrm{IIIc}}$ were used. This was done to prevent any delamination front propagation and assess the distribution of the SERR. Then, simulations of the full DCB test were performed, using a straight delamination front (like the one shown in Figure 2) and a maximum applied displacement of 15 mm. The remaining numerical parameters used in this work are reported in Table 2. Finally, a standard Abaqus simulation with the in-built crack propagation algorithm using VCCT was also performed, as a reference.

DOI : 10.60691/yj56-np80
https://gem.ec-nantes.fr/en/eccm21-proceedings/

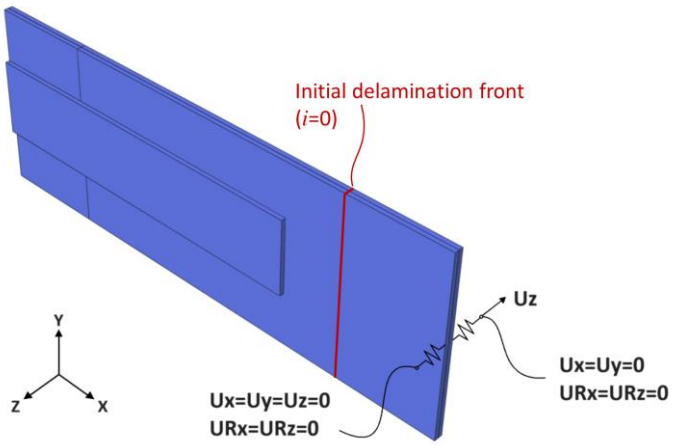

Figure 2. Partially reinforced DCB with boundary conditions.

Table 1. Material properties of the carbon/epoxy unidirectional laminas (moduli are in GPa, fracture toughnesses are in kJ/m^2, Poisson's ratios and η are dimensionless) [3].

E_1	E_2=E_3	G_{12}=G_{13}	G_{23}	ν_{12}=ν_{13}	ν_{23}	$\mathcal{G}_{Ic}$	$\mathcal{G}_{IIc}$	$\mathcal{G}_{IIIc}$	η
154	8.5	4.2	3.036	0.35	0.4	0.305*	2.77*	2.77*	2.0866

*These values are multiplied by 10^3 for the analyses with unrealistically high fracture toughnesses.

Table 2. Numerical parameters used in the validation case (note that a displacement is applied to the simulation, rather than a load).

P_{max} (mm)	ΔP (mm)	d_n (mm)	n_{poly}	n_{sim}
15	1	0.5	12	15

3. Results and discussion

3.1. Simulation without propagation

Figure 3a shows the experimental delamination front mapped on a standard mesh and then remeshed using the developed algorithm. As shown in Figure 3b, the newly developed mesh is able to eliminate the SERR concentrations, resulting in a smooth distribution. As shown, the discontinuities in the standard mesh causes peaks in the SERR, thus resulting in a premature delamination propagation. These peaks are mitigated in the smoothed crack front, resulting in a delayed, more realistic propagation.

DOI : 10.60691/yj56-np80
https://gem.ec-nantes.fr/en/eccm21-proceedings/

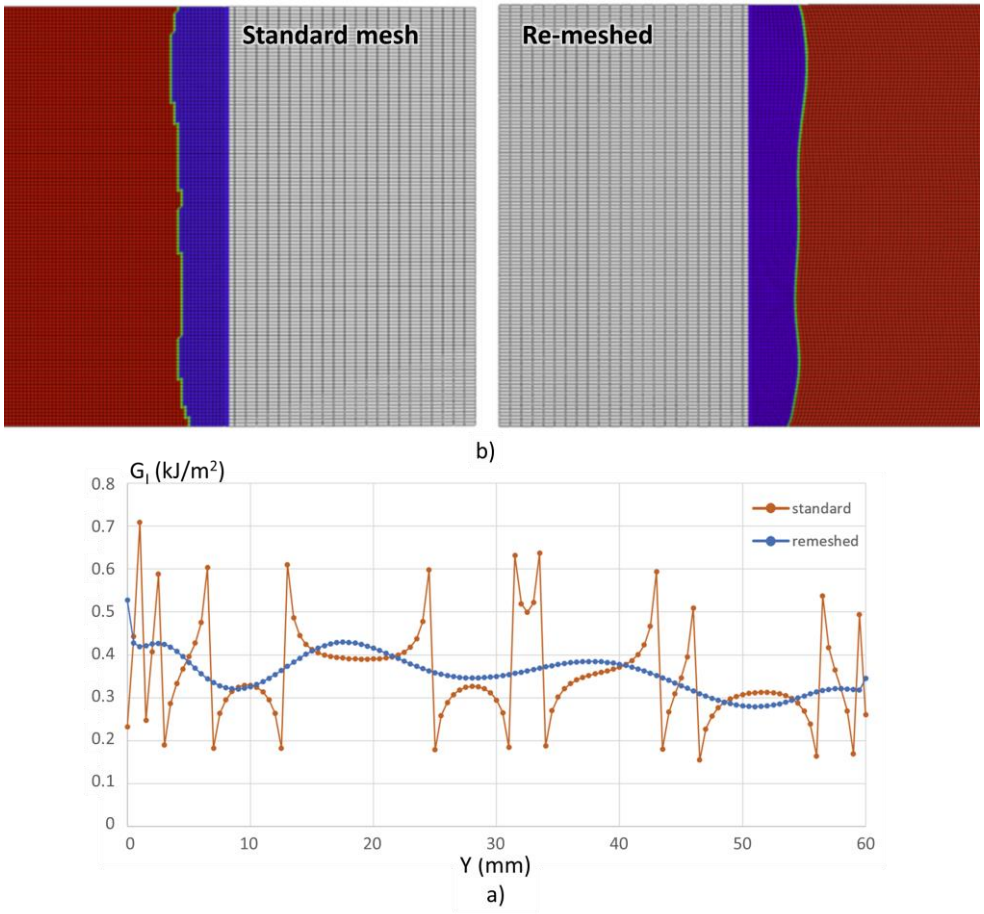

Figure 3. a) Standard and remeshed delamination front and b) distributions of the SERR.

3.2. Full test simulations

Figure 4a compares the experimental load displacement curve with the ones obtained with the different modelling approaches, namely the standard and the one implementing the remeshing algorithm. As shown, the reduction of the SERR concetration did not improve significantly the predictions of the standard simulation approach. In both cases, a large load drop is recorded slightly after 10 mm of opening displacement. As shown in Figure 4b, this is associated to a significant advancement of the delamination front.

To further investigate the reason for such discrepancy, no-propagation simulations were performed with the experimental delamination front reported for 12 mm of applied displacement. Like for the previous case reported in Section 3.1, the delamination front was mapped on a regular mesh and then smoothed with the developed algorithm. Both fronts were simulated. The resulting SERR distributions are reported in Figure 5 and compared with the fracture toughness $\mathcal{G}_{\mathrm{Ic}}$. As shown, the remeshed algorithm is still able to ensure a smoother and continuous distribution of the SERR. However, in both cases the SERR reports values higher than $\mathcal{G}_{\mathrm{Ic}}$.

DOI : 10.60691/yj56-np80
https://gem.ec-nantes.fr/en/eccm21-proceedings/

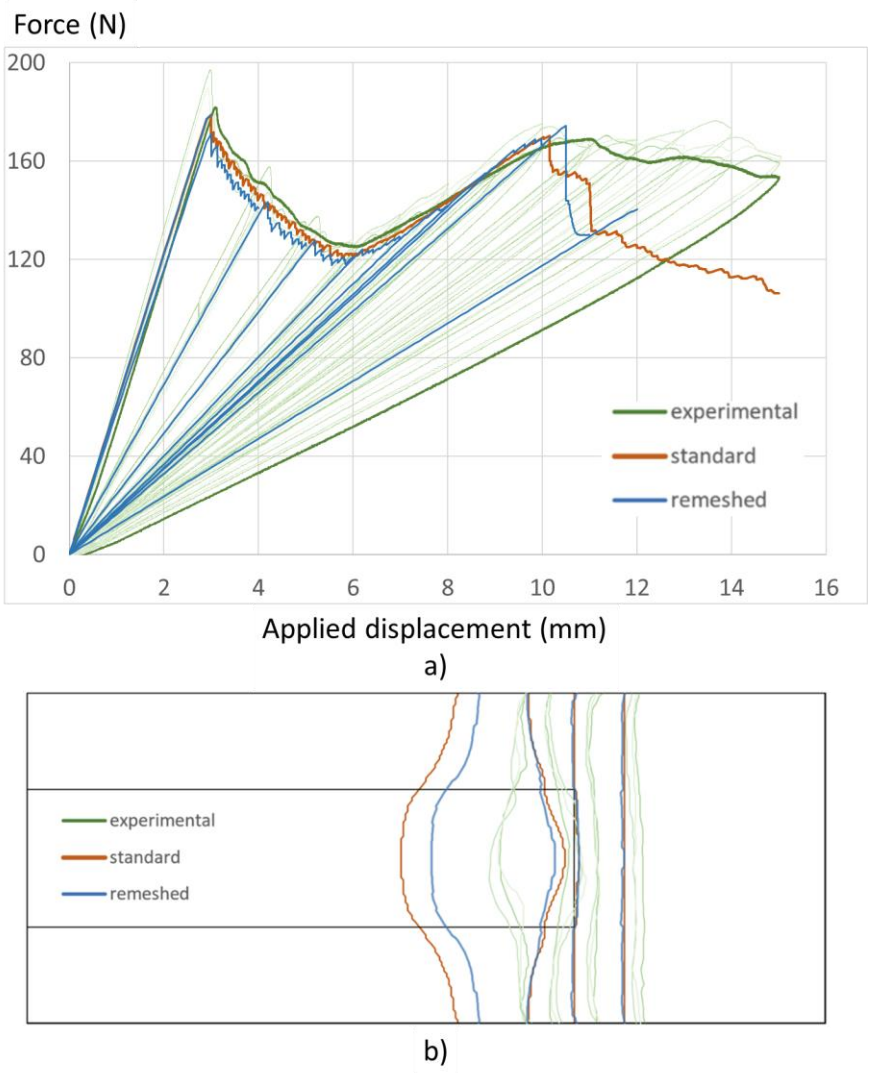

Figure 4. Comparison of results of the tests and numerical simulations, with the standard approach and with the remeshing algorithm: a) load-displacement curves and b) distribution fronts.

Figure 5 thus shows that, according to the simulations, the experimentally observed delamination front should not be possible. Two possible explanations exist for such incompatibility. First, Carreras et al. [7] showed how a cohesive zone model they developed could capture the correct propagation of the delamination front. While cohesive elements can model the process zone ahead of the delamination front, this is not possible with VCCT, which is a linear elastic fracture mechanics approach [1]. Therefore, neglecting the non-linear behaviour ahead of the delamination front could lead to these significant discrepancies. A second explanation for such incompatibility could be related to fibre bridging. The occurrence of such phenomenon can result in an increased fracture toughness $\mathcal{G}_{\mathrm{Ic}}$. An increasing $\mathcal{G}_{\mathrm{Ic}}$ during the test could explain why the fist stages of the test are predicted quite accurately (see Figure 4a), while inaccuracies occur at the later stages, when bridging is fully developed.

In both cases, the versatility of the sequential simulations approach could be exploited to cope with such inaccuracies as future development. First of all, a non-linear release of the bonded nodes could tentatively be used to simulate the process zone ahead of the delamination front [8]. Moreover, the Python master script is able to manipulate the Abaqus input files, thus imposing different fracture

DOI : 10.60691/yj56-np80
https://gem.ec-nantes.fr/en/eccm21-proceedings/

toughness for different simulations: this would allow the implementation of an evolving fracture toughness during the entire analysis.

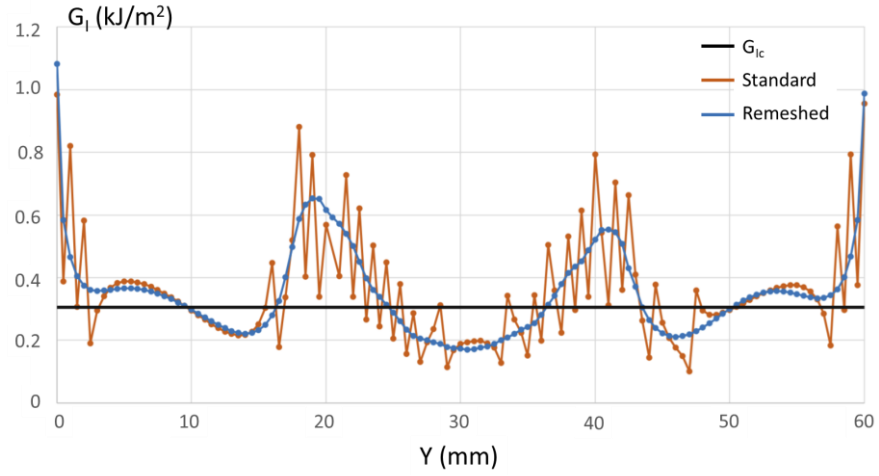

Figure 5. SERR distributions for the experimental delamination front reported at 12 mm of applied displacement.

4. Conclusions and future works

This work presented a new remeshing algorithm to automatically generate meshes conformal to delamination front in numerical simulations. This was done aiming at improving the applicability of the VCCT in simulations featuring large and curved delamination fronts. The algorithm was implemented in a sequential simulations approach, which was previously developed for fatigue analyses. The application of the algorithm to a reference case showed that it was effective in mitigating the SERR peaks. Nevertheless, insignificant improvement was observed for the selected validation case. This was mainly attributed to either the lack of a non-linear process zone or the consideration of the bridging effect on the composite's fracture toughness.

Future developments will thus aim to improve the prediction of the static propagation by addressing these issues, exploiting in particular the versatility of the sequential simulations approach. A further development consists in the implementation of the remeshing algorithm in the already developed fatigue approach, namely the sequential-static-fatigue approach [2].

Acknowledgments

Dr. Laura Carreras and Prof. Albert Turon (Universidad de Girona) are gratefully acknowledged for their insights and clarifications on the experimental validation case.

References

[1] Pascoe, J. A., Alderliesten, R. C., Benedictus, R., Methods for the prediction of fatigue delamination growth in composites and adhesive bonds – A critical review, Engineering Fracture Mechanics, **112**–**113**, 2013, p. 72–96.

[2] Martulli, L. M., Bernasconi, A., An efficient and versatile use of the VCCT for composites delamination growth under fatigue loadings in 3D numerical analysis: the Sequential Static Fatigue algorithm, International Journal of Fatigue, **170**, 2023, p. 107493.

[3] Carreras, L., Renart, J., Turon, A., Costa, J., Bak, B. L. V., Lindgaard, E., Martin de la Escalera, F., Essa, Y., A benchmark test for validating 3D simulation methods for delamination growth under quasi-static and fatigue loading, Composite Structures, **210**, 2019, p. 932–941.

[4] Benzeggagh, M. L., Kenane, M., Measurement of mixed-mode delamination fracture toughness

DOI : 10.60691/yj56-np80

of unidirectional glass/epoxy composites with mixed-mode bending apparatus, Composites Science and Technology, **56**, 1996, p. 439–449.

[5] Dassault Systemès, Abaqus 2021 manual.

[6] Raimondo, A., Dávila, C. G., Bisagni, C., Cohesive analysis of a 3D benchmark for delamination growth under quasi-static and fatigue loading conditions, Fatigue and Fracture of Engineering Materials and Structures, **45**, 2022, p. 1942–1952.

[7] Carreras, L., Bak, B. L. V., Jensen, S. M., Lequesne, C., Xiong, H., Lindgaard, E., Benchmark test for mode I fatigue-driven delamination in GFRP composite laminates: Experimental results and simulation with the inter-laminar damage model implemented in SAMCEF, Composites Part B: Engineering, **253**, 2023, p. 110529.

[8] De Carvalho, N. V., Mabson, G. E., Krueger, R., Deobald, L. R., A new approach to model delamination growth in fatigue using the Virtual Crack Closure Technique without re-meshing, Engineering Fracture Mechanics, **222**, 2019, p. 106614.